JOC Article

A New Class of Linear Tetrapyrroles: Acetylenic 10,10a-Didehydro-10a-homobilirubins

Bin Tu, Brahmananda Ghosh, and David A. Lightner*

Department of Chemistry, University of Nevada, Reno, Nevada 89557

lightner@scs.unr.edu

Novel bilirubin analogues with dipyrrinones conjoined to an acetylene rather than a methylene group were synthesized and examined spectroscopically. Despite the increased separation of the dipyrrinones forced by replacing a $-CH_2-$ by a $-C{\equiv}C-$ unit, molecular dynamics calculations show that, like bilirubin, they may still engage in intramolecular hydrogen bonding to carboxylic acid groups when the propionic acid chains are slightly lengthened, e.g., butanoic acids. Unlike bilirubin, however, which is bent in the middle and has a ridge-tile shape, the acetylene orients the attached dipyrrinones along a linear path, and intramolecular hydrogen bonding preserves a *twisted linear molecular shape*. The extended planes of the dipyrrinones intersect along the $-C{\equiv}C-$ axis at an angle of 136° for the conformation stabilized by intramolecular hydrogen bonding in the bis-butyric acid rubin (**1b**). With shorter acid chains (propionic), only one CO_2H can engage an opposing dipyrrinone in intramolecular hydrogen bonding, and in this energy-minimum conformation of the linear pigment **1a**, the intersection of the extended planes of the dipyrrinones has an angle of 171°. Spectroscopic evidence for such linearized and twisted structures was found in the pigments' NMR spectral data and their exciton UV−vis and induced circular dichroism spectra.

Introduction

Bilirubin (Figure 1A), the yellow neurotoxic pigment of jaundice,[1,2] is a member of a class of compounds called "linear tetrapyrroles",[3] as distinct from cyclic tetrapyrroles, such as porphyrins. Linear tetrapyrroles such as bilirubin and its biogenetic precursor (blue-green) biliverdin are formed copiously in healthy mammals by catabolism of hemoglobin and other heme proteins (Figure 1B),[1−3] but are the structures really linear? Fischer determined their constitutional structures by degradation methods and total synthesis and provided linear structure representations without designating the configurational stereochemistry at the C(4) and C(15) double bonds—and C(10) in biliverdin.[3,4] In 1939, Lemberg[5] suggested that the 4Z, 10Z, and 15Z double-bond configurations should follow logically from those of the porphyrin precursor, thus making the porphyrin-like representations of Figure 1B more likely. However, in his classic (1949) book[6] with Legge, Lemberg used "linear" representations, apparently since they "save space and are more readily visualized." Linear structures for bilirubin and biliverdin persist in biochemistry texts, usually with the wrong (E) double-bond stereochemistry, and such inaccurate representations continue to find their way into scientific articles.[7] The Z-configuration was shown 20−25 years ago, and we now know that (4Z,10Z,15Z)-verdins and (4Z,15Z)-rubins are bent in the middle.[8,9] The former adopt a porphyrin-like conformation,[3] but the latter (whose dipyrrinones may in principle rotate freely about the central 10-CH_2) fold into a ridge-tile shape stabilized by intramolecular hydrogen bonding between the propionic acids and the opposing dipyrrinones.[9,10]

Verdins and rubins are bent in the middle because their dipyrrinones are conjoined to sp^2- and sp^3-hybridized carbons (C-10, Figure 1), respectively. However, if the dipyrrinones were joined to sp-hybridized carbons,

(1) (a) McDonagh, A. F. Bile pigments: Bilatrienes and 5, 15-biladienes. In *The Porphyrins*; Dolphin, D., Ed.; Academic Press: New York, 1979; Vol. VI, Chapter 6. (b) Schmid, R.; McDonagh, A. F. Hyperbilirubinemia. In *The Metabolic Basis of Inherited Disease*, 4th ed.; Stanbury J. B., Wyngaarden J. B., Fredrickson D. S., Eds.; McGraw-Hill: New York, 1978; pp 1221−1257.

(2) Chowdhury, J. R.; Wolkoff, A. W.; Chowdhury, N. R.; Arias, I. M. Hereditary jaundice and disorders of bilirubin metabolism. In *The Metabolic and Molecular Bases of Inherited Disease*; Scriver C. F., Beaudet A. L., Sly W. S., Valle D., Eds.; McGraw-Hill: New York, 2001; Chapter 125, pp 3063−3101.

(3) Falk, H. *The Chemistry of Linear Oligopyrroles and Bile Pigments*; Springer-Verlag: Wien, 1989.

(4) Fischer, H.; Plieninger, H. *Hoppe-Seyler's Z. Physiol. Chem.* **1942**, *274*, 231−260.

(5) Lemberg, R. *Austral. Chem. Int. J.: Proc.* **1939**, *6*, 170−180.

(6) Lemberg, R.; Legge, J. W. *Hematin Compounds and Bile Pigments*; Interscience Publ., Inc.: New York, 1949.

(7) (a) Barañano, D. E.; Rao, M.; Ferris, C. D.; Snyder, S. H. *Proc. Natl. Acad. Sci. U.S.A.* **2002**, *99*, 16093−16098. (b) Ritter, S. *Chem. Eng. News*, Dec 9, 2002, p 6. (c) McDonagh, A. F.; Lightner, D. A.; Snyder, S. H. *Chem. Eng. News*, Feb 3, 2003, p 2. (d) Frankenburg, N.; Lagarias, J. D. *J. Biol. Chem.* **2003**, *278*, 9219−9220.

(8) (a) Sheldrick, W. S. *Isr. J. Chem.* **1983**, *23*, 155−166. (b) Sheldrick, W. S. *J. Chem. Soc., Perkin Trans. 2* **1976**, 1457−1462.

(9) (a) Bonnett, R.; Davies, J. E.; Hursthouse, N. B.; Sheldrick, G. M. *Proc. R. Soc. London, Ser. B* **1978**, *202*, 249−268. (b) LeBas, G.; Allegret, A.; Mauguen, Y.; DeRango, C.; Bailly, M. *Acta Crystallogr., Sect. B* **1980** *B36*, 3007−3011. (b) Becker, W.; Sheldrick, W. S. *Acta Crystallogr., Sect. B* **1978**, *B34*, 1298−1304.

(10) Person, R. V.; Peterson, B. R.; Lightner, D. A. *J. Am. Chem. Soc.* **1994**, *116*, 42−59.
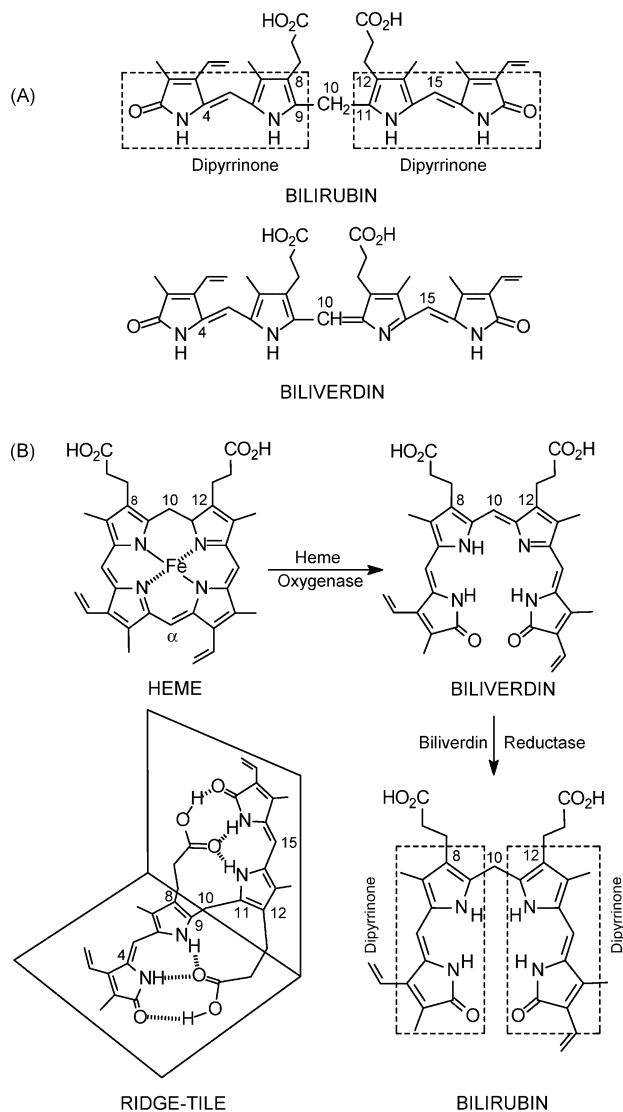
FIGURE 1. (A) Linear representations of bilirubin and biliverdin. (B) Formation of bilirubin and biliverdin from heme. The most stable conformation of biliverdin is porphyrin-like and helical. The most stable conformation of bilirubin is neither linear nor porphyrin-like but shaped like a ridge-tile and stabilized by intramolecular hydrogen bonding.

i.e., a $-C\equiv C-$ group, they would be constrained to lie on a linear path. Yet, little is known of 10-homologated rubins, and the known examples are not necessarily forced to be linear. Six years ago, we published on the first (yellow) 10a-homorubin[11] (Figure 2), and a year earlier a few simple examples of a new class of (red) dehydro-10a-homorubins, also called *b*-homoverdins, were synthesized.[12] Subsequently a didehydro-10a-homorubin or dehydro-*b*-homoverdin (also red), was prepared.[12b] These types of tetrapyrroles are bent in the middle, although the (10*E*)-*b*-homoverdin may have a more or less linear shape, as might (9*E*,10a*E*)-dehydro-*b*-homoverdin. A 10a-homorubin has more degrees of freedom
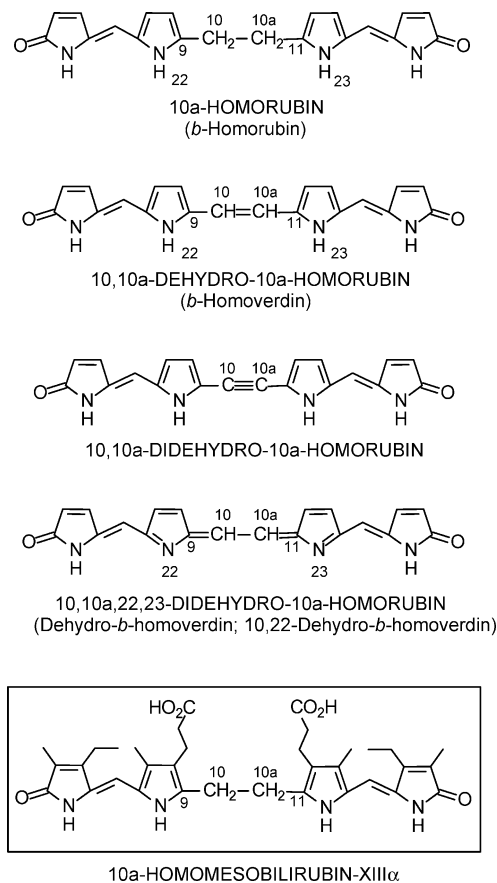
(11) Pfeiffer, W. P.; Lightner, D. A. *Tetrahedron Lett.* **1994**, *35*, 9673−9676.

(12) (a) Chen, Q.-Q.; Ma, J.-S.; Wang, C.-Q.; Liu, Y.-Y.; Yan F.; Cheng, L.-J.; Jin, S.; Falk, H. *Monatsh. Chem.* **1995**, *126*, 983−991. (b) Chen, Q.-Q.; Falk, H. *Monatsh. Chem.* **1995**, *126*, 1097−1107.

FIGURE 2. Homorubin/homoverdin skeletons and the only known homorubin (in box).

about the 9−10−10a−11 C−CH$_2$−CH$_2$−C segment, and the lone example (10a-homomesobilirubin-XIIIα)[11] is bent in the middle and intramolecularly hydrogen bonded.[11] In contrast, an acetylene analogue, 10,10a-didehydro-10a-homomesorubin-XIIIα, would have a $-C\equiv C-$ core and would be isoelectronic and tautomeric with 10,10a,-22,23-didehydro-10a-homorubin (dehydro-*b*-homoverdin); yet it cannot bend in the middle and should thus be "linear."

In the following, we describe the synthesis, conformation and spectroscopic properties of the first linear bilirubin analogues (**1**) with the 10-CH$_2$ group replaced by $-C\equiv C-$ (Figure 3). Molecular models indicate that such novel rubins possessing butyric acids (**1b**) at C(8) and C(12) can undergo intramolecular hydrogen bonding with the CO$_2$H groups fitting nicely into a bilirubin-like (Figure 1B) intramolecular hydrogen-bonding motif by engaging the dipyrrinones. With propionic acids (**1a**), however, the acid chains are too short to permit *both* CO$_2$H groups to engage an opposing dipyrrinone in intramolecular hydrogen bonding; thus, both **1a** and **1b** serve as useful comparative models for analyses of linear and linearly twisted bilirubins.

Results and Discussion

Synthesis. From our perspective, the simplest route to the preparation of acetylenic rubins **1a** and **1b** was to follow the "1 + 2 + 1" approach[13] outlined in Scheme 1, where an α,α′-diformyldipyrrolylacetylene (**2a** or **2b**) is
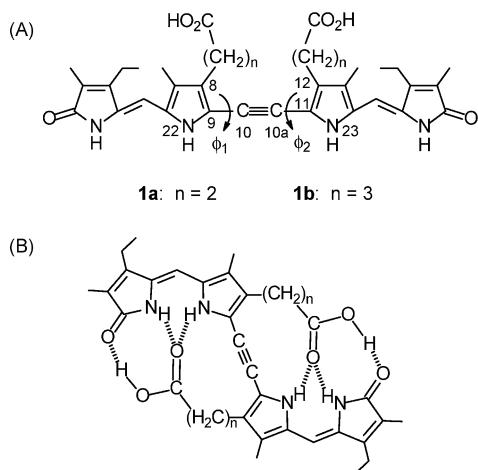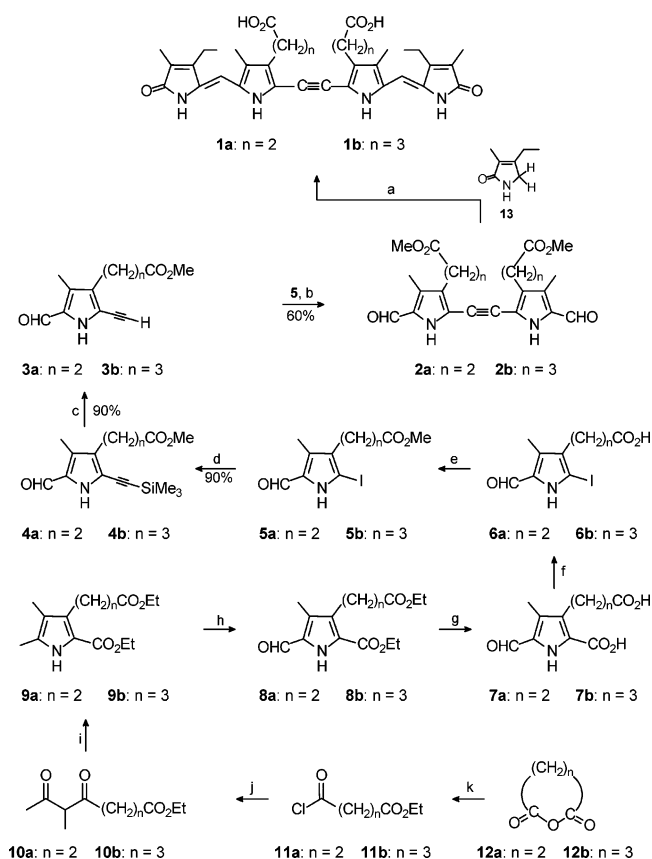
(A)

1a: n = 2   **1b**: n = 3

(B)

FIGURE 3. (A) Linear and (B) intramolecularly hydrogen-bonded representations of acetylenic bilirubin analogues **1a** and **1b**, with the usual central CH_2 of bilirubin at C(10) replaced by an acetylene unit. Rotations about the ϕ_1 and ϕ_2 torsion angles [N(22)−C(9)−C(10)−C(10a) and C(10)−C(10a)−C(11)−N(23), respectively] interconvert the major important conformations.

coupled with two equivalent of a pyrrolinone (e.g., **13**). The strategy has been used successfully in the syntheses of 10-oxobilirubin[14] and various end-ring-modified bilirubins.[15] The required pyrrolinone (**13**) had been prepared previously;[14] the required dipyrrole acetylenes (**2a** and **2b**) were unknown, but simpler analogues absent alkanoic acid groups had been reported previously in connection with porphyrinoid syntheses.[16] Construction of the dipyrrole acetylenes **2a** and **2b** thus followed the general procedure wherein iodopyrroles **6a** and **6b** were used to prepare acetylene pyrroles **3a** and **3b**—and also coupled with them. But iodopyrroles **6** had not been reported previously. The precursors to **7a** (**8a**[17] and **9a**[18]) were known from work in our laboratory; the equivalent precursors (**8b** and **9b**) to **7b** had not been reported, nor had diketo ester **10b**, whose analogue (**10a**) was used in the preparation of **9a**.[18]

Diketo ester **10b** was prepared from glutaric anhydride (**12b**) as outlined in Scheme 1. Thus, reaction with ethanol and then thionyl chloride afforded the half-ester-acid chloride **11b**, which was used to acylate the TMS enol ether of 2-butanone. A Fischer−Knorr-type reaction of **10b** with diethyl oximinomalonate in the presence of Zn and acetic acid afforded pyrrole **9b** in 51% yield. Oxidation of the α-methyl of **9b** using CAN[19] gave **8b** in 60% yield. Iodine was introduced at the other α-position

(13) Boiadjiev, S. E.; Lightner, D. A. *Synlett* **1994**, 777−785.

(14) Chen, Q.; Huggins, M. T.; Lightner, D. A.; Norona, W.; McDonagh, A. F. *J. Am. Chem. Soc.* **1999**, *121*, 9253−9264.

(15) (a) Brower, J. O.; Lightner, D. A.; McDonagh, A. F. *Tetrahedron* **2000**, *56*, 7869−7883. (b) Brower, J. O.; Lightner, D. A.; McDonagh, A. F. *Tetrahedron* **2001**, *57*, 7813−7827.

(16) (a) Cho, D. H.; Lee, J. H.; Kim, B. H. *J. Org. Chem.* **1999**, *64*, 8048−8050. (b) Martire, D. O.; Jux, N.; Aramendia, P. F.; Negri, R. M.; Lex, J.; Braslavsky, S.; Schaffner, K.; Vogel, E. *J. Am. Chem. Soc.* **1992**, *114*, 9969−9978.

(17) Kar, A.; Lightner, D. A. *Tetrahedron* **1998**, *54*, 5151−5170.

(18) Trull, F. R.; Franklin, R. W.; Lightner, D. A. *J. Heterocycl. Chem.* **1987**, *24*, 1573−1579.

(19) (a) Bobál, P.; Lightner, D. A. *J. Heterocycl. Chem.* **2001**, 1219−1221. (b) Thyrann, T.; Lightner, D. A. *Tetrahedron Lett.* **1996**, *37*, 315−318.

SCHEME 1[a]

1a: n = 2   **1b**: n = 3   **13**

3a: n = 2   **3b**: n = 3   **2a**: n = 2   **2b**: n = 3

4a: n = 2   **4b**: n = 3   **5a**: n = 2   **5b**: n = 3   **6a**: n = 2   **6b**: n = 3

9a: n = 2   **9b**: n = 3   **8a**: n = 2   **8b**: n = 3   **7a**: n = 2   **7b**: n = 3

10a: n = 2   **10b**: n = 3   **11a**: n = 2   **11b**: n = 3   **12a**: n = 2   **12b**: n = 3

[a] Reagents and conditions: (a) $KOH/CH_3OH−H_2O$, reflux; (b) $Pd(PPh_3)_2Cl_2$, CuI, diethylamine, 50 °C; (c) Bu_4NF THF, rt; (d) $Pd(PPh_3)_2Cl_2$, CuI, TMS-acetylene Et_2NH, 50 °C; (e) CH_2N_2, CH_3OH; (f) I_2, KI, $KHCO_3−H_2O$; (g) $LiOH−H_2O$, THF−H_2O, 70 °C; (h) CAN, HOAc−THF−H_2O; (i) Zn, HOAc, H_2O; (j) CH_2=C-$(OSiMe_3)CH_2CH_3$, $ZnCl_2$, CH_2Cl_2; (k) (i) ethanol, (ii) $SOCl_2$.
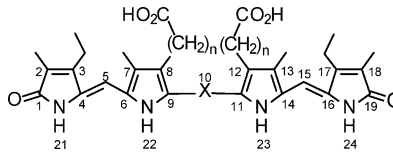
following saponification using $LiOH \cdot H_2O$ at 70 °C in aq THF (to give **7b** from **8b** and **7a** from **8a**) and treatment with I_2−KI in aqueous bicarbonate to afford **6a** and **6b**. (Iodination using ICl at 80 °C in acetic acid was not successful.) After esterification of the propionic acids with CH_2N_2, the iodine was replaced (in **5**) in >80% yield by TMS-acetylene using $Pd(PPh_3)_2Cl_2$−CuI catalyst in Et_2-NH. The resulting acetylenes (**4a** and **4b**) were deprotected using *n*-Bu_4NF to provide **3a** and **3b**, which were coupled (Sonogashira[20]) to their respective iodopyrrole precursors (**5a** and **5b**) in 40−60% yield using $Pd(PPh_3)_2$-Cl_2−CuI catalyst to afford the requisite α,α′-diformyl-dipyrrolylacetylenes **2a** and **2b**. Reaction of **2a** or **2b** with excess pyrrolinone **13** in hot aqueous-methanolic KOH over 60 h gave the desired acetylenic rubins **1a** and **1b** in 30−40% yield.

Structure. The constitutional structures of **1** and **2** follow from the method of synthesis (Scheme 1) and from their ^{13}C NMR spectra (Table 1). When compared with ^{13}C NMR data[15a] from the known mesobilirubin-XIIIα (MBR-XIII), the various carbons of the dipyrrinone(s) of **1a** and **1b** have counterparts with recognizably similar chemical shifts. The major differences are found at

(20) Sonogashira, K.; Tohda, Y.; Hagihara, N. *Tetrahedron Lett.* **1975**, 4467−4470.

TABLE 1. Comparison of ^{13}C NMR Chemical Shift Assignments[a] for Acetylenic Bilirubin Analogues 1a (X = C≡C, *n* = 2) and 1b (X = C≡C, *n* = 3) with Mesobilirubin-XIIIα (MBR-XIII, X = CH₂, *n* = 2) (CD₃)₂SO

	C-13 chemical shifts[a]		
position	**1a**	**1b**	MBR-XIII[b]
1,19-CO	172.6	172.6	171.8
2,18	124.8	124.7	122.9
2,18-CH₃	9.57	9.57	9.14
3,17	147.7	147.7	147.2
3,17-CH₂	17.56	17.56	17.15
3²,17²-CH₃	15.08	15.16	14.81
4,16	131.6	130.9	127.8
5,15-CH=	96.54	96.68	97.69
6,14	126.0	126.0	122.4
7,13	122.1	122.2	122.0
7,13-CH₃	8.50	8.50	8.07
8,12	129.0	129.6	119.2
8¹-CH₂	20.08	24.36	19.25
8²-CH₂	34.98	25.85	34.56
8³-CH₂	-	33.60	-
8,12-CO₂H	174.1	174.7	174.0
9,11	114.1	114.3	130.3
10[a](10[b])	87.12	87.09	23.34

[a] δ in ppm downfield from (CH₃)₄Si. Assignments by HMBC and HMQC. [b] From ref 15a.

carbons that are attached (C(9,11)) or close (C(8,12)) to the acetylenic carbons and found to be ∼16 ppm more shielded and ∼10 ppm more deshielded, respectively, relative to C(9,11) and C(8,12) in MBR-XIII. Far smaller differences (∼2 ppm relative deshieldings) are found at C(2,18), C(4,16), and C(4,16) that alternate along pathway of conjugated C=C bonds.

Conformation, Solution, and Chromatographic Properties. The sp carbons of the acetylene unit dictate a linear pigment geometry, with any bending coming principally from the sp² carbons 5 and 15 in the middle of each dipyrrinone (Figure 3). Unlike biliverdins, however, the dipyrrinone units of **1a** and **1b** may rotate freely and independently about the acetylene(s), thereby creating numerous rotational isomers. In some conformations, one or both dipyrrinones are brought into sufficiently close proximity for intramolecular hydrogen bonding to the carboxylic acid groups, given the appropriate length of the alkanoic acid chain.

In bilirubin and mesobilirubin-XIIIα, propionic acid chains enjoy optimal intramolecular hydrogen bonding (Figure 1),[9,21,22] but butyric acid chains are also found to engage the dipyrrinones in hydrogen bonding.[21,22] When the chains are too long or too short, the pigment polarity increases: greatly with acetic acid chains and (counterintuitively) substantially with pentanoic and hexanoic

TABLE 2. Comparison of the Dipyrrinone NH and Carboxylic Acid OH Chemical Shifts[a] of Acetylenic Rubins 1a and 1b with Those of Mesobilirubin-XIIIα in CDCl₃ and (CD₃)₂SO Solvents

	CDCl₃			(CD₃)₂SO		
pigments	lactam NH	pyrrole NH	CO₂H	lactam NH	pyrrole NH	CO₂H
1a				10.11	11.18	12.14
1b	10.30	9.30	13.20	10.00	11.04	12.03
MBR XIII	10.57	9.15	13.62	9.72	10.27	11.87

[a] δ in ppm downfield from (CH₃)₄Si.

acid chains.[21] With chain lengths mismatched for intramolecular hydrogen bonding, the pigments typically exhibit increased polarity (on TLC and HPLC), decreased solubility in CHCl₃ and increased solubility in dilute aqueous bicarbonate.

Unlike their bright yellow parent, mesobilirubin-XIIIα, acetylenic rubins **1a** and **1b** are red solids that form orange solutions. Analogue **1a** is insoluble in most nonpolar organic solvents such as chloroform, dichloromethane, and even in CH₃OH. In contrast, **1b** exhibits limited solubility in chloroform and dichloromethane, indicating that it is less polar than **1a**. In accord with these observations, on silica gel TLC using 4% by vol. CH₃OH in CH₂Cl₂ as eluent, **1a** has an R_f ∼ 0.21, and **1b** has an R_f ∼ 0.6, conditions where MBR-XIII exhibits an R_f ∼0.85. Somewhat contradictorily, the retention time of **1a** (17.1 min) lies between that of **1b** (12.5 min) and MBR-XIII (18.3 min) on reversed-phase HPLC. Consistent with intramolecular hydrogen bonding in both **1a** and **1b**, and similar to bilirubin and mesobilirubin-XIIIα, neither analogue is extracted into 5% (or saturated) aqueous sodium bicarbonate from chloroform. Clearly, the change of the central −CH₂− to −C≡C− does not have a large effect on the chloroform/bicarbonate partition coefficient. Taken collectively, these data suggest the presence of intramolecular hydrogen bonding in **1a** and **1b**.

Conformation from ^{1}H NMR Spectroscopy. Consistent with these predictions, **1b** is found to be sufficiently soluble in CHCl₃ for ^{1}H NMR measurements; unfortunately, **1a** was insufficiently soluble. The ^{1}H NMR spectrum of **1b** reveals dipyrrinone NH chemical shifts (Table 2) characteristic of intramolecular hydrogen bonding to a carboxylic acid. Dipyrrinones are known to be avid participants in hydrogen bonding, preferably to carboxylic acids,[23,24] but secondarily to each other (with association constants ∼30 000 M⁻¹ in CDCl₃).[25] In CDCl₃, dipyrrinone monomers exhibit lactam and pyrrole NH chemical shifts of ∼8 ppm,[25b] whereas intermolecularly hydrogen-bonded dipyrrinone dimers typically exhibit lactam and pyrrole NH chemical shifts ∼11 and ∼10 ppm, respectively. Dipyrrinones hydrogen bonded to CO₂H groups typically show lactam and pyrrole NH

(21) (a) Lightner, D. A.; Person, R. V.; Peterson, B. R.; Puzicha, G.; Pu, Y.-M.; Bojadziev, S. *Biomolecular Spectroscopy II*; Birge, R. R., Nafie, L. A., Eds.; Proc. SPIE *1432*, **1991**, 2−13. (b) Shrout, D. P.; Puzicha, G.; Lightner, D. A. *Synthesis* **1992**, 328−332. (c) Trull, F. R.; Person, R. V.; Lightner, D. A. *J. Chem. Soc., Perkin Trans. 2* **1997**, 1241−1250.

(22) Dörner, T.; Knipp, B.; Lightner, D. A. *Tetrahedron* **1997**, *53*, 2697−2716.

(23) (a) Boiadjiev, S. E.; Anstine, D. T.; Lightner, D. A. *J. Am. Chem. Soc.* **1995**, *117*, 8727−8736. (b) Boiadjiev, S. E.; Anstine, D. T.; Maverick, E.; Lightner, D. A. *Tetrahedron: Asymmetry* **1995**, *6*, 2253−2270.

(24) (a) Huggins, M. T.; Lightner, D. A. *J. Org. Chem.* **2000**, *65*, 6001−6008. (b) Huggins, M. T.; Lightner, D. A. *Tetrahedron* **2001**, *57*, 2279−2287.

(25) (a) Huggins, M. T.; Lightner, D. A. *Monatsh. Chem.* **2001**, *132*, 203−221. (b) Nogales, D. F.; Ma, J.-S.; Lightner, D. A. *Tetrahedron* **1993**, *49*, 2361−2372.
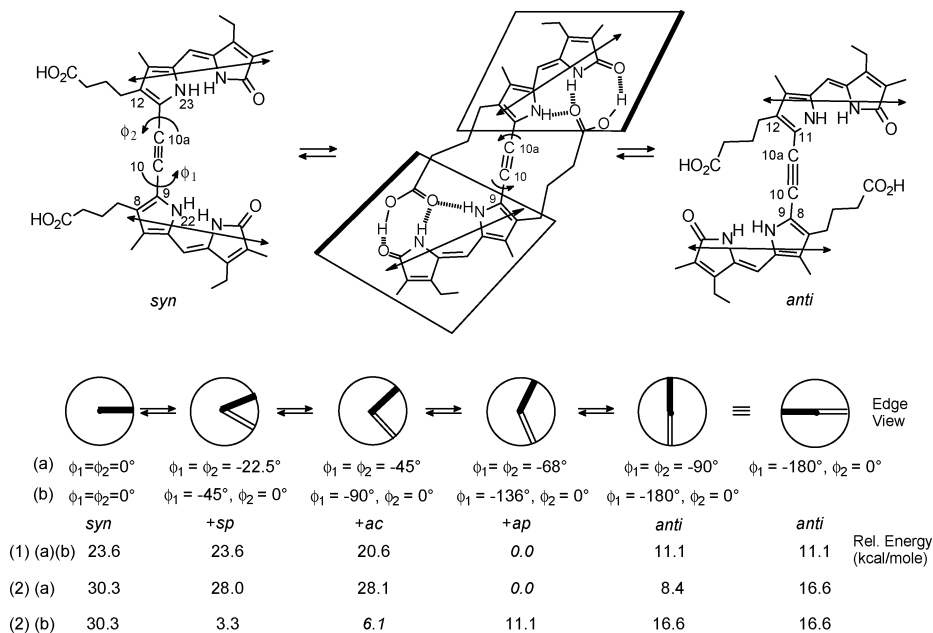
FIGURE 4. Interconversion of conformations of **1b** by rotation about torsion angles $\phi_1 = N(22)-C(9)-C(10)-C(10a)$] and $\phi_2 = C(9)-C(10)-C(10a)-N(23)$ as viewed edgewise from the $C(2)-C(3)-C(5)-C(7)$ dipyrrinone backbone. The dark bar represents the long edge of the lower dipyrrinone; the open bar represents an edge view of the top dipyrrinone. In the eclipsed syn conformation, ϕ_1 and ϕ_2 are defined as 0°. The $(-)$ rotations about ϕ_1 and ϕ_2 depicted interconvert the planar syn and anti conformations. (An enantiomeric set of twisted conformations ($\phi_1 = \phi_2 \neq 0° \neq 90°$) is created by $(+)$ rotations.) The relative energies associated with the designated conformers are shown below each. The $\phi_1 = \phi_2 = -68°$ global energy-minimum conformation is stablized by intramolecular hydrogen bonding. Other combinations of rotations about ϕ_1 and ϕ_2, e.g., $\phi_1 = 0°$, $\phi_2 = 180°$ also interconvert the syn and anti conformations. In rotations (a), the ϕ torsion angles are driven so that $\phi_1 = \phi_2$; in (b) ϕ_2 is held at 0° and ϕ_1 is driven from 0° to $-180°$. In (1), the $C(9)-C(10)-C(11)$ torsion angle is constrained to be 180°; so that (a) and (b) track through identical conformers, and $E(-68°, -68°) = -6.42$ kcal/mol. In (2), the $C(9)-C(10)-C(10a)-C(11)$ angle is unconstrained and this leads to differing conformations, e.g., $\phi_1 = \phi_2 = -90$, and $\phi_1 = -180°$, $\phi_2 = 0°$. Here, $E(-68°, -68°) = -13.52$ kcal/mol. The approximate locations of the dipyrrinone long-wavelength electric dipole transition moments lie along the long axis of the chromophore, as indicated.

chemical shifts of ~10.5 and ~9 ppm.[24] This particular shielding of the pyrrole NH seems to be diagnostic of intramolecular hydrogen bonding, and in Table 2, one finds a pyrrole chemical shift of 9.30 ppm for **1b** as compared with the 9.15 ppm value seen in MBR-XIII. The deshielding of the CO_2H to 13.20 ppm provides added support to our conclusion that **1b** adopts an intramolecularly hydrogen-bonded conformation (Figure 3). Unfortunately, the lesser solubility of **1a** in $CDCl_3$ made it impossible to draw a similar conclusion for its conformation. The greater solubility of **1b** in $CDCl_3$ allowed for $^1H\{^1H\}$-homonuclear NOE experiments, which showed the expected NOEs between the pyrrole and lactam NHs, and between the $C(5,15)$ olefinic hydrogens and the $C(7,-13)$ methyls and $C(3,17)$ ethyls. Only a faint NOE could be seen between the CO_2H and lactam NH, which suggests weaker hydrogen bonding in **1b** than in bilirubin or mesobilirubin-XIIIα. In $(CD_3)_2SO$, both **1a** and **1b** exhibited many of the same NOEs seen above, characteristic of the syn-*Z* configuration of the dipyrrinones.

Conformation Analysis from Molecular Dynamics. Independent rotations of the approximately planar, thermodynamically most stable *syn-Z*-dipyrrinones of **1a** or **1b** about the acetylene unit (about ϕ_1 and ϕ_2, as illustrated for **1b** in Figure 4) lead to an infinite number of conformations, including two high energy limiting cases where the dipyrrinones lie coplanar: the syn and anti (Figure 4). Lying between these extremes is a

conformation stabilized by intramolecular hydrogen bonding, given sufficient length of the alkanoic acid substituents at $C(8)$ and $C(12)$. In comparing **1a** and **1b**, molecular models and molecular dynamics calculations[26] show a better match for intramolecular hydrogen bonding with butyric acids (**1b**) than with propionic acids (**1a**): both CO_2H groups of **1b** are engaged in intramolecular hydrogen bonding to an opposing dipyrrinone; in **1a** only one CO_2H can become engaged. The energy-minimum conformation of **1a**, as determined by molecular dynamics using the Sybyl force field, gave a conformation in which only one of the propionic acid groups is engaged in intramolecular hydrogen bonding to an opposing dipyrrinone (Figure 5). To achieve such limited hydrogen bonding, the structure is torqued in such a way as to exclude hydrogen bonding between the remaining propionic acid and dipyrrinone. However, lengthening both acid chains to butyric (**1b**) is sufficient to allow both CO_2H groups to engage in intramolecular hydrogen bonding to the opposing dipyrrinones. In the energy-minimized structures of **1a** and **1b**, the extended planes of the dipyrrinones of each intersect along the $-C\equiv C-$

(26) The molecular dynamics calculations used to find the global energy minimum conformations of **1** were run on an SGI Octane workstation using vers. 6.9 of the Sybyl force field as described in ref 10. The ball and stick drawings were created from the atomic coordinates using Müller and Falk's "Ball and Stick" program for the Macintosh (http://www.orc.uni-Linz.ac.at/mueller/ball_stick.html).
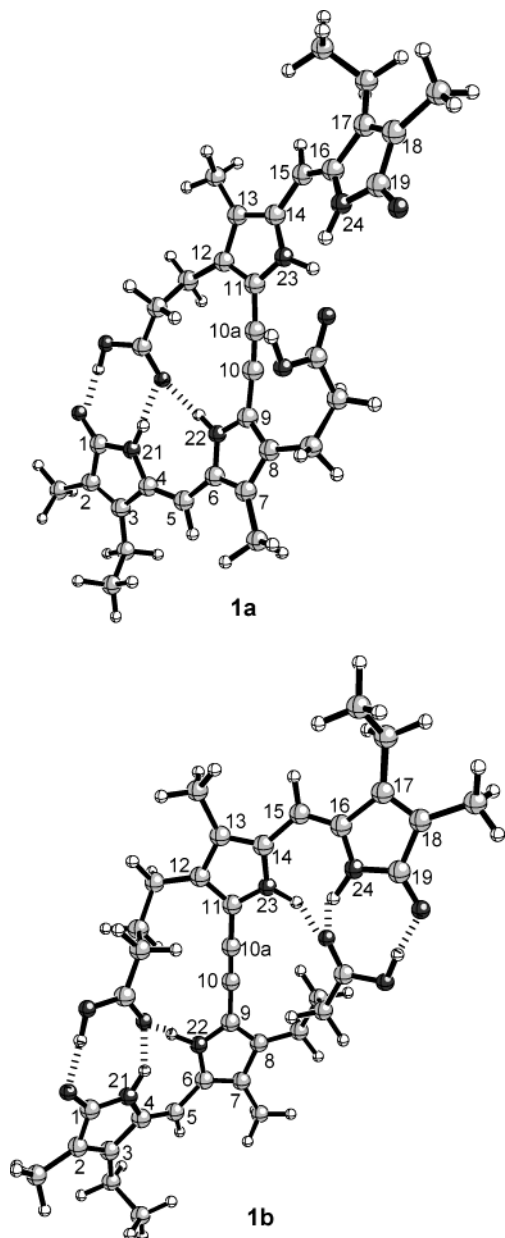
FIGURE 5. Ball and stick representations of the energy-minimum conformations of **1a** and **1b**, as determined by molecular dynamics using the Sybyl force field. In this **1a**, ϕ_1 ($N_{22}-C_9-C_{10}-C_{10a}$) = 53°, ϕ_2 ($N_{23}-C_{11}-C_{10a}-C_{10}$) = 118°, ϕ_3 ($C_9-C_{10}-C_{10a}-C_{11}$) = −16°, ψ_1 ($C_4-C_5-C_6-N_{22}$) = −25°, ψ_2 ($N_{23}-C_{14}-C_{15}-C_{10}$) = −27°, $C_9-C_{10}-C_{10a} = C_{10}-C_{10a}-C_{11}$ = 176°, $N_{22}-C_9-C_{10}$ = 121°, $C_{10a}-C_{11}-N_{23}$ = 125°. In this **1b**: $\phi_1 = \phi_2$ = −68°, ϕ_3 = −16°, $\psi_1 = \psi_2$ = 26°, $C_9-C_{10}-C_{10a} = C_{10}-C_{10a}-C_{11}$ = 176°, $N_{22}-C_9-C_{10} = C_{10a}-C_{11}-N_{23}$ = 122°.

axis. In **1b**, the extended planes of the dipyrrinones intersect at a 136° angle; in **1a**, the angle of intersection is 171°.

In **1a** and **1b**, rotations about ϕ_1 and ϕ_2 [illustrated for **1b** in (a) of Figure 4], as well as rotations about ϕ_1 while holding $\phi_2 = 0°$ (or vice versa) [illustrated for **1b** in (b) of Figure 4], interconvert planar syn and anti conformers by rotating through twisted conformations. When the $C(9)-C(10)-C(10a)$ and $C(10)-C(10a)-C(11)$ bond angles are fixed at 180° [(1) of Figure 4] in order to maintain strict linearity of $C(9)-C(10)-C(10a)-C(11)$, these two

types of rotations [(a) and (b)] generate identical structures, i.e., the conformer with $\phi_1 = \phi_2 = -45°$ is identical to that at $\phi_1 = -90°$, $\phi_2 = 0°$ (or $\phi_1 = 0°$, $\phi_2 = -90°$), and the conformer at $\phi_1 = \phi_2 = -90°$ ($\phi_1 = \phi_2 = +90°$) is identical to that at $\phi_1 = 180°$, $\phi_2 = 0°$ (or $\phi_1 = 0°$, $\phi_2 = 180°$). For **1b**, the conformer at $\phi_1 = \phi_2 = -68°$ (identical to that at $\phi_1 = -136°$, $\phi_2 = 0°$) is found to lie at the global energy minimum because in this conformation each dipyrrinone and an opposing CO_2H group are fully engaged in intramolecular hydrogen bonding.

When the constraint $C(9)-C(10)-C(10a) = C(10)-C(10a)-C(11) = 180°$ is relaxed, the $\phi_1 = \phi_2 = -68°$ conformer lies at an even lower global energy minimum (−13.52 vs −6.42 kcal/mol) due to even more effective intramolecular hydrogen bonding afforded by bending $C(9)$ and $C(11)$ out of strict linearity with the triple bond, in such a way that the $C(9)-C(10)-C(10a)$ and $C(10)-C(10a)-C(11)$ bond angles do not necessarily bend in the same plane, i.e., the $C(9)-C(10)-C(10a)-C(11)$ torsion angle (ϕ_3) is no longer 0°, but 16° (Table 3). Lifting the linearity restriction causes the $C(9)-C(10)-C(10a)$ and $C(10)-C(10a)-C(11)$ bond angles to bend as much as ∼8° and the dipyrrinone twist angles (ψ_1 and ψ_2, Table 3) to twist more or less severely in the energy minimization. One interesting consequence of lifting strict linearity of $C(9)-C(10)-C(10a)-C(11)$ grouping is that conformations such as $\phi_1 = \phi_2 = -90°$ and $\phi_1 = \phi_2 = -68°$ no longer correspond to ($\phi_1 = -180°$, $\phi_2 = 0°$) and ($\phi_1 = -136°$, $\phi_2 = 0°$), respectively (Table 3), due to a differing ability to participate in intramolecular hydrogen bonding. When linearity about the acetylene group is lifted, the $C(9)$ and $C(11)$ atoms do not necessarily bend out of linearity in the same plane, i.e., $\phi_3 \neq 0°$. This means that although the $C(9)-C(10)-C(10a)$ and $C(10)-C(10a)-C(11)$ angles may bend away from 180° to the same extent, e.g., to 175° in both the ($\phi_1 = \phi_2 = -90°$) and in ($\phi_1 = -180°$, $\phi_2 = 0°$) conformers, $C(9)$ and $C(11)$ in the former bend out of linearity in the same plane ($\phi_3 = 0.3°$), but in the latter they do not ($\phi_3 = -30°$); hence, the conformers are not identical. The various conformers of Table 3 are shown in ball and stick[26] representations in Figure 6, where structural identities of ($\phi_1 = \phi_2 = -22.5°$) and ($\phi_1 = -45°$, $\phi_2 = 0°$), ($\phi_1 = \phi_2 = 45°$) and ($\phi_1 = -90°$, $\phi_2 = 0°$), etc., of the pairs in data set 1a,b are evident. Likewise, the structural dissimilarities of the corresponding "pairs" of data set 2a,b are evident in their ball and stick conformational representations (Figure 7).

Conformation from UV−vis Spectral Analysis. Additional evidence on the conformation of **1a** and **1b** comes from solvent-dependent UV−vis spectra. Over a wide range of solvents with varying polarity and hydrogen-bonding ability (benzene, chloroform, acetone, methanol, acetonitrile, and dimethyl sulfoxide), the UV−vis spectra of **1a** and **1b** show greater solvent-dependence than their parent rubin, MBR-XIII (Table 4). Compared with their parent rubin (with broad absorption near 430 nm and a shoulder near 395 nm in most solvents), acetylene rubins **1a** and **1b** showed a wider separation of long wavelength and shorter wavelength bands. These long-wavelength absorptions are probably exciton in nature and correspond to the two exciton components from electric dipole−electric dipole transition moment interaction of the two dipyrrinone chromophores.

TABLE 3. Conformations of 1b As Determined by Torsion Angles ϕ and ψ,[a] and the Relative Energies

data set[a,b]	ϕ_1 (22−9−10−10a)	ϕ_2 (10−10a−11−23)	ψ_1 (4−5−6−22)	ψ_2 (23−14−15−16)	ϕ_1 (22−9−10−10a)	ϕ_2 (10−10a−11−23)	ϕ_3 (9−10−10a−11)	ΔE^c (kcal/mol)
(1a,b)	0	0	33	11.5	−180	−180	0	23.6
(1a,b)	−22.5	−22.5	26.3	26.3	−45	0	0	23.6
(1a,b)	−45	−45	26.5	26.3	−90	0	0	20.6
(1a,b)	−68	−68			−136	0	0	0
(1a,b)	−90	−90	26.3	26.3	−180	0	0	11.1
(2a)	0	0	31.7	30.6			104	30.3
(2a)	−22.5	−22.5	37	37			−28	28
(2b)			20	22	−45	0	−98	3.3
(2a)	−45	−45	39	37			−81	28.1
(2b)			26.5	35.6	−90	0	−70	6.1
(2a)	−68	−68	26.4	26.4			16	0
(2b)			22	22	−136	0	−27	11.1
(2a)	−90	−90	23	22			0.3	8.4
(2b)			36	37	−180	0	−30	16.6

[a] Refer to Figure 4 for numbering and reference systems used. In (1), the 9−10−10a and 10−10a−11 bond angles are fixed at 180°; in (2), the computed bond angles 9−10−10a and 10−10a−11 are all 171−177°. In (1), the computed bond angles 22−9−10 and 10a−11−23 lie between 119.4° and 121.9°; in (2), they lie between 119° and 125°. [b] Data set (1) refers to conformations in which linearity is maintained along $\phi_3 = 9−10−10a−11 = 180°$, e.g., 9−10−10a and 10−10a−11 are fixed at 180°. In data set (2), this restriction is lifted. In (a), ϕ_1 and ϕ_2 are driven so that $\phi_1 = \phi_2$; in (b), ϕ_2 is held at 0° and ϕ_1 is driven from 0° to −180°. [c] ΔE of (1) is relative to the $\phi_1 = \phi_2 = −68°$ energy minimum of −6.42 kcal/mol; ΔE of (2) is relative to the $\phi_1 = \phi_2 = −68°$ energy minimum of −13.52 kcal/mol. Thus, all values of (1) are ∼7 kcal/mol higher energy than the corresponding (ϕ_1, ϕ_2) conformers of (2).

In exciton coupling theory, the relative orientation of the relevant electric dipole transition moments is very important.[10,27] For dipyrrinones, this transition dipole lies along the long axis of the chromophore.[28,29] When linked to an acetylene, the dipyrrinones may rotate into a large number of relative orientations (conformations), e.g., Figures 4 and 6. There are two limiting planar conformations, syn and anti. In the (planar) anti conformer (Figure 4), the dipyrrinone long-wavelength electric dipole transition moments associated with the ∼420 nm UV−vis absorption of the dipyrrinone chromophore lie parallel and in-line (Figures 4 and 8). In the syn, they lie in the same plane and oblique. The planar conformations are achiral, and the relevant dipyrrinone electric dipole transition moments lie in a common plane. However, there are many other conformations, all chiral, originating by rotating the dipyrrinones about the −C≡C− axis. In such conformations, the planes encompassing each dipyrrinone are not coincident and thus the dipyrrinone electric dipole transition moments have a chiral, helical ("oblique", Figure 7) relative orientation. For the twisted conformers, exciton coupling theory thus predicts intensity from both exciton transitions and hence a broadened UV−vis absorption curve. This is seen in the UV−vis spectra of both 1a and 1b in $(CH_3)_2SO$ solvent, where the location (λ) and shape of the UV−vis absorptions are very similar − and similar also to the UV−vis spectrum of mesobilirubin-XIIIα (MBR-XIII) in $(CH_3)_2SO$.

The UV−vis absorption characteristics of MBR-XIII are little altered in going from polar $(CH_3)_2SO$ solvent to nonpolar solvents such as chloroform and benzene−an indication that the ridge-tile conformation (or more particularly the relative orientation of the dipyrrinone electric dipole transition moments) is scarcely altered with changes in solvents. A similar behavior is seen in UV−vis data from 1a (Table 4), which suggests that oblique orientations of the dipyrrinone electric dipole transition moments are maintained in the solvents studied. Exactly which twisted conformations are obtained is unclear. In contrast, 1b shows distinct solvatochromism, whereupon changing from $(CH_3)_2SO$ to nonpolar, hydrogen-bond-promoting solvents, the long-wavelength exciton component grows at the expense of the short wavelength. This behavior is consistent with selection of a more anti-like conformation, with an intramolecularly hydrogen-bonded conformation, where the dipyrrinone transition moments lie more "in-line" (Figure 8), as might be seen in the global energy minimum conformation ($\phi_1 = \phi_2 = −68°$, Figures 4, 6, and 7).

Induced Circular Dichroism. Bilirubins fold in the middle into ridge-tile conformations that lie at energy minima. With the added stabilization from intramolecular hydrogen bonding, two interconverting conformational enantiomers (Figure 9) dominate the conformational energy map.[10] In isotropic solvents, a 50:50 mixture of enantiomers is obtained, but when a chiral complexation agent, such as quinine[29] or serum albumin,[30] is added, the equilibrium shifts toward either the **M** or **P** enantiomer, and in such cases one observes typically intense bisignate circular dichroism (CD) Cotton effects for the long-wavelength rubin UV−vis electronic transitions near 400−450 nm. Such Cotton effects are associated with an exciton interaction between the rubin's two dipyrrinone choromphores that are not directly conjugated,[10,29] and the signed order of the Cotton effects has been correlated with the relative orientation of the dipyrrinones and hence the absolute configuration **M** or **P** of the rubin.[10,29]

The acetylenic rubins of this work cannot be folded into ridge-tile shapes. Rather, in 1b, intramolecular hydrogen bonding (Figure 10) preserves a linear, rotated conforma-

(27) Kasha, M.; El-Bayoumi, M. A.; Rhodes, W. J. Chim. Phys.-Chim. Biol. 1961, 58, 916−925.

(28) (a) Falk, H.; Vormayr, G.; Margulies, L.; Metz, S.; Mazur, Y. Monatsh. Chem. 1986, 117, 849−858. (b) Falk, H.; Grubmayr, K.; Höllbacher, G.; Hofer, O.; Leodolter, A.; Neufingerl, F.; Ribó, J. M. Monatsh. Chem. 1977, 108, 1113−1130.

(29) Lightner, D. A.; Gawroński, J. K.; Wijekoon, W. M. D. J. Am. Chem. Soc. 1987, 109, 6354−6362.

(30) Lightner, D. A.; Wijekoon, W. M. D.; Zhang, M. H. J. Biol. Chem. 1988, 263, 16669−16676.
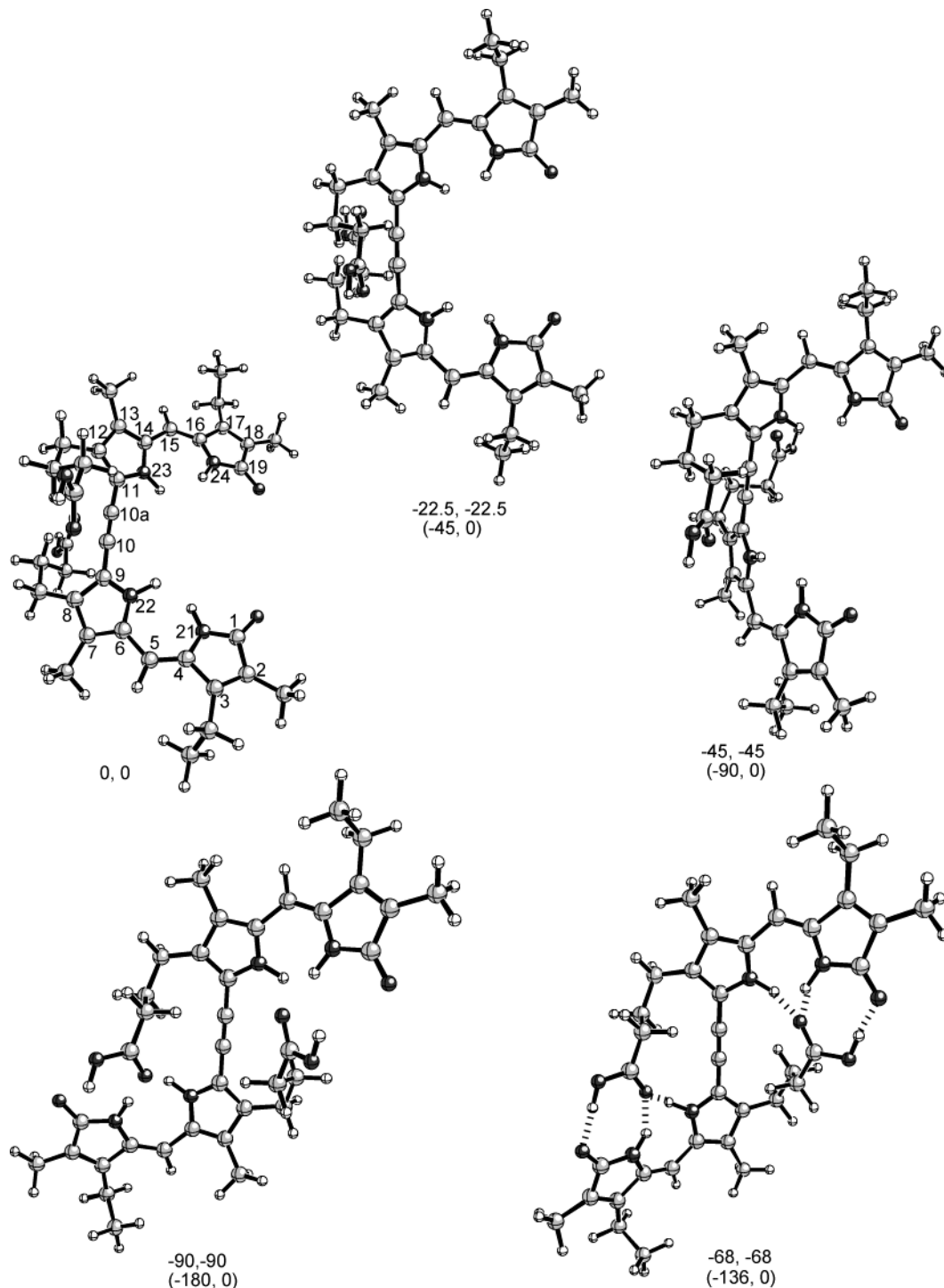
FIGURE 6. Ball and stick representations of the conformations of **1b** depicted in Figure 4.

tion. As the two dipyrrinones approach the coplanarity of the anti conformation (Figure 4), the orientation of the relevant electric transition dipoles tends toward the "in line" orientation, as in the intramolecularly hydrogen-bonded structures (Figure 4). In such conformations, the long-wavelength component of the exciton couplet is expected to dominate—as may be noted in the UV−vis spectrum of **1b** in CHCl$_3$. As seen by CD, **1b** in CHCl$_3$ with added quinine[29] affords a very broad positive Cotton effect near 540 nm and broad Cotton effect near 390 nm,

with |Δε| ∼ 15−28 (Figure 11). The data are consistent with the *ap* (or anti) conformations reflecting probably the near planarity of the two dipyrrinones. In contrast, **1a** exhibits a more obvious and more intense exciton chirality CD, with a long-wavelength position Cotton effect near 440 nm (Δε +59) and a shorter wavelength negative Cotton effect near 390 nm (Δε −92). The data suggest that twisted conformation dominates the CD spectrum of **1a** and has a positive helical orientation of the relevant dipyrrinone electric dipole transition mo-
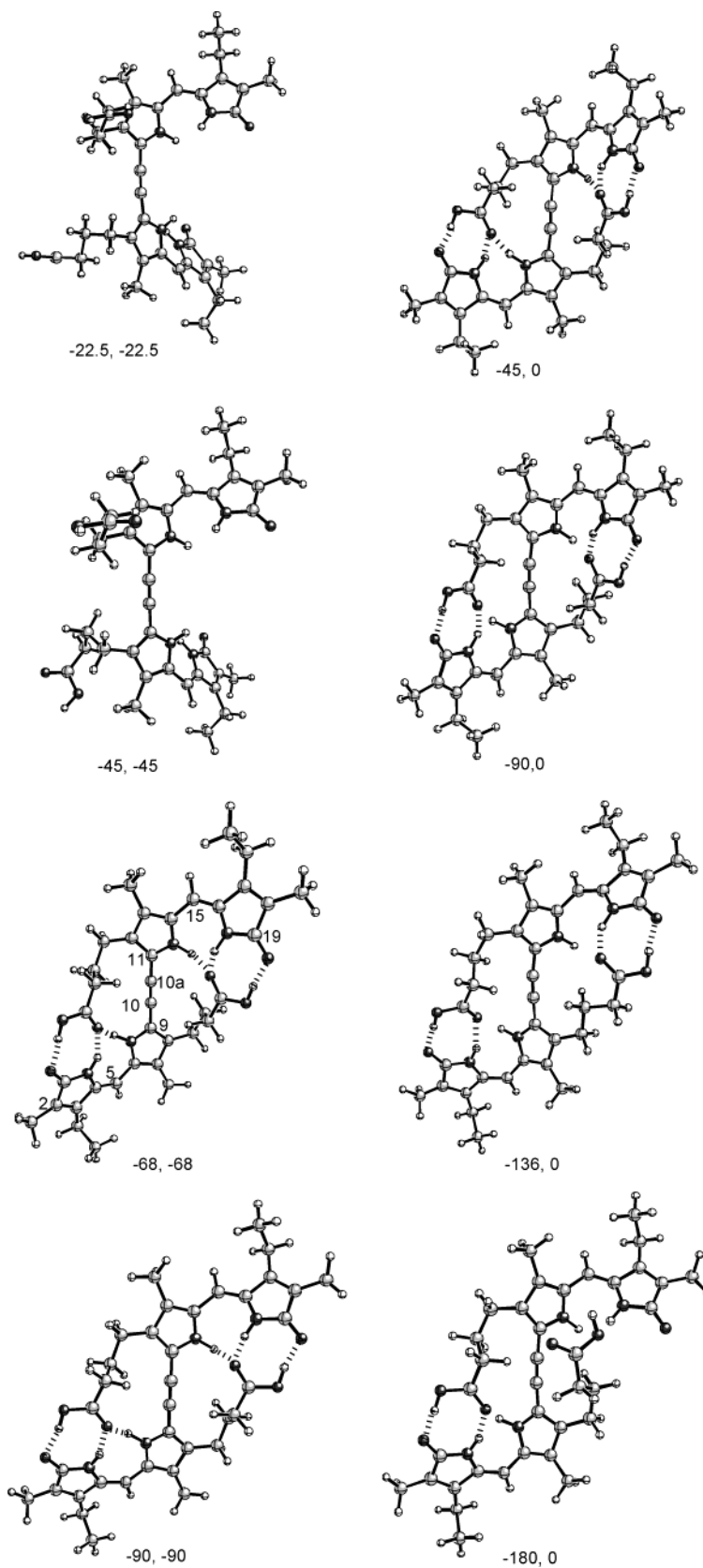
FIGURE 7. Representative examples of the differing conformations (in ball and stick, representation, ref 26) of data sets 2a (left column, $\phi_1 = \phi_2$) and 2b (right column, $\phi_1 = x°$, $\phi_2 = 0°$) of Figure 4 and Table 3.

ments, as predicted by exciton chirality theory[31] (see Figure 7) and consistent with the $+ac$ conformation of Figure 4.

In pH 7.4 aqueous buffered human serum albumin (HSA), **1a** exhibits a negative chirality bisignate CD curve with a broad negative ($\Delta\epsilon$ −26) Cotton effect near

TABLE 4. Solvent-Dependence of the UV−Vis Spectral Data[a] of Acetylenic Rubins 1a and 1b with Mesobilirubin-XIIIα (MBR -XIII)

	ϵ^{max} (λ^{max}, nm)					
compd	benzene	CHCl₃	(CH₃)CO	CH₃OH	CH₃CN	(CH₃)₂SO
1a	40 200 (444)	36 700 (484)	43 900 (437)	44 500 (452)	41 400 (436)	45 800 (440)
	40 500 (388)[b]	26 100 (407)[b]	36 800 (384)[b]	31 400 (392)[b]	33 800 (386)[b]	41 000 (389)[b]
1b	48 800 (533)	57 900 (542)	50 700 (512)	46 400 (497)	52 300 (512)	39 900 (442)
	13 900 (396)[b]	53 300 (515)[b]	14 400 (393)[b]	19 600 (396)[b]		37 500 (389)[b]
MBR-XIII	49 000 (439)	50 300 (431)	49 700 (427)	50 600 (425)	49 000 (425)	52 500 (428)
bilirubin	45 800 (447)	46 920 (450)	47 600 (447)	45 300 (446)	47 000 (445)	47 800 (446)
			34 600 (415)[b]	37 500 (416)[b]	39 400 (417)[b]	37 700 (415)[b]

[a] At 22 °C in concentrations ~1.4 × 10⁻⁵ M, λ^{max} in nm, ϵ^{max} in L·mol⁻¹ cm⁻¹. *[b]* Shoulders (or) inflections were determined by first- and second-derivative spectra.
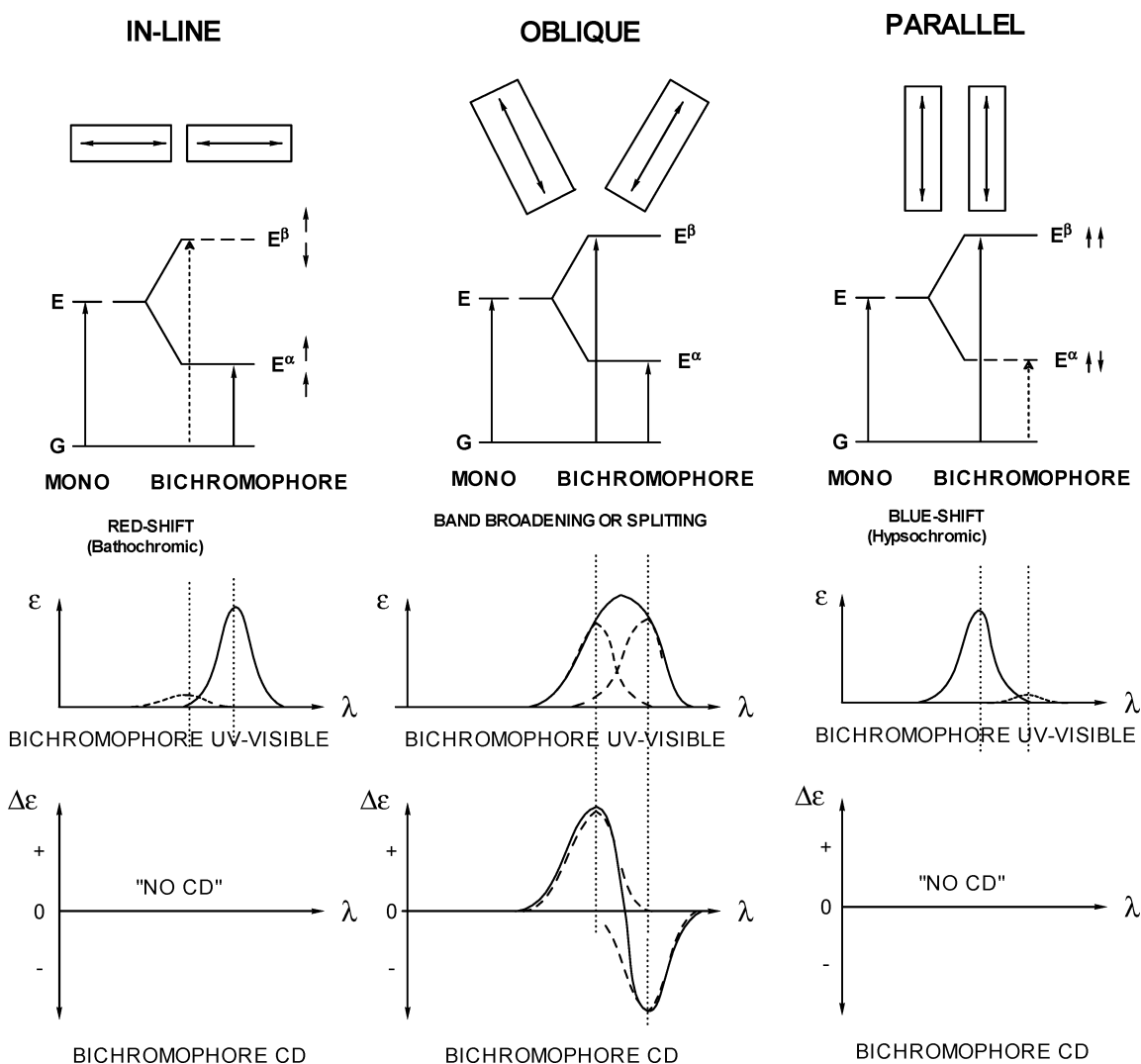

FIGURE 8. Exciton splitting diagrams (upper) and predicted UV−vis and CD spectra (lower) for the three "limiting" case geometrical arrangements of the electric transition moments: linear, oblique (of which there are many possible), and parallel. The in-line orientation is found in the planar, intramolecularly hydrogen-bonded structure of Figure 3. The oblique case is found in a vast array of folded or helical conformations most notably in the *M* and *P* ridge-tile conformations (Figure 1) by the porphyrin-like conformation. The consequences of the three differing alignments of the electric transition dipoles in the bichromophore may be seen in the differing UV−vis and CD spectra. An arbitrary signed order for the CD couplet is shown. According to exciton chirality theory, a bisignate CD with the long-wavelength negative−short-wavelength positive Cotton effects shown here would indicate a left-handed or *M*-helical orientation of the transition dipoles. A long-wavelength positive and short-wavelength negative bisignate CD couplet corresponds to a *P*-helical orientation. Redrawn from ref 10. Copyright 1994 American Chemical Society.

495 nm and a sharper Cotton effect ($\Delta\epsilon$ +67) near 390 nm. Complexation of a +*sc* or +*ac* twisted conformation of **1a** is apparently preferred. In contrast, acetylene rubin

1b also shows a better-resolved positive chirality bisignate CD, with $\Delta\epsilon$ +37 near 465 nm and $\Delta\epsilon$ −69 near 390 nm. The striking difference in the signed order of the
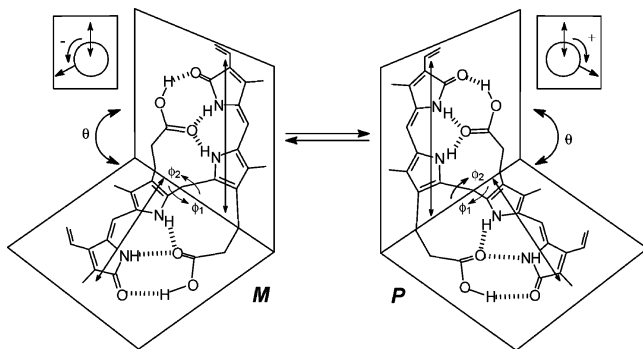
FIGURE 9. Ridge-tile shaped, folded intramolecularly hydrogen-bonded enantiomeric conformations of bilirubin (***M*** and ***P***). Interconversion (***M*** ⇌ ***P***) is accomplished by rotating about ϕ_1 and ϕ_2. In ***M*** and ***P***, the dipyrrinone chromophores are planar, and the angle of intersection of the two planes (dihedral angle, θ) is ~100° for $\phi_1 \sim \phi_2 \sim 60°$. The double-headed arrows represent the approximate direction and intensity of the dipyrrinone long wavelength electric transition dipole moments. The relative orientations or helicities (***M***, minus; ***P***, plus) of the vectors are shown (inset) for each enantiomer. For these conformations the ***M*** dipole helicity correlates with the ***M*** molecular chirality and the ***P*** helicity with the ***P*** molecular chirality. Redrawn from ref 10. Copyright 1994 American Chemical Society.

bisignate Cotton effects of **1a** and **1b** is a clear indication of differences in conformation and chirality of the pigments complexed to HSA. Whether one can attribute such a difference to the greater facility for engaging in intramolecular hydrogen bonding in **1b** vs **1a** is as yet unclear, but likely. In this connection, it may be noted that both the mesobilirubin-XIIIα with propionic acids replaced by butyric acids and mesobilirubin-XIIIα itself engage in conformation-determining intramolecular hydrogen bonding. The latter exhibits a well-defined positive chirality exciton coupling bisignate CD ($\Delta\epsilon_{436}^{max}$ +37, $\Delta\epsilon_{388}^{max}$ -42) but the former exhibits only a broad, indistinct negative chirality bisignate CD ($\Delta\epsilon_{420}^{max}$ −16, $\Delta\epsilon_{420}^{max}$ +8).[21c]

Experimental Section

General Procedures. Nuclear magnetic resonance (NMR) spectra were obtained at 300 MHz unless otherwise noted or on a 500 MHz spectrometer. HMQC, HMBC, and NOE NMR were obtained at 500 MHz. Chemical shifts were reported in δ ppm referenced to the residual CHCl$_3$ ^{1}H signal at 7.26 ppm and ^{13}C at 77.23 ppm. Analytical thin-layer chromatography (TLC) was carried out on silica gel IB-F plates (125 μm layers). Flash column chromatography was carried out using silica gel, 60−200 mesh. HPLC analyses were carried out with a detector at 410 on an Ultrasphere-IP 5 μm C-18 ODS column (25 × 0.46 cm) fitted with a similary-packed precolumn (4.5 × 0.46 cm). The flow rate was 0.75−1.0 cm^3/min; the elution solvent was 0.1 M di-*n*-octylamine acetate in 5% aqueous CH$_3$OH; the column temperature was ~34 °C. Spectroscopic data were obtained in spectral grade solvents.

UV and CD Measurements. Stock solutions of **1a** and **1b** (~7.0 × 10^{-4} M) were prepared by dissolving an appropriate amount of the desired pigment in 2 mL of DMSO. Next, a 100 μL aliquot of the stock solution was diluted to 5 mL (volumetric flask) the specified organic solvent for UV−vis studies (Table 4), or for CD studies involving human serum albumin (HSA), with an HSA solution (~2.8 × 10^{-5} M in pH 7.4 Tris buffer). The final concentration of the solution was ~1.4 × 10^{-5} M in pigment. Up to four 5 mL solutions of each pigment were prepared, as needed, in 5 mL volumetric flasks. For CD studies in CHCl$_3$, solutions were prepared directly in CHCl$_3$ containing a 300:1 molar ration of quinine/pigment to give final concentrations of ~1.4 × 10^{-5} M in pigment.

Ethylsuccinoyl chloride (11a) and ethylglutaroyl chloride (11b) were prepared in yields of 92% and 90% from succinic anhydride and glutaric anhydride, **12a** and **12b**, respectively, by reaction first with with absolute ethanol, then (after removing the ethanol) with thionyl chloride.[32] The TMS silyl enol ether of 2-butanone was prepared according to the literature.[33] Methyl 4,6-dioxo-6-methylheptanoate (**10a**) was prepared in 50% yield as described below for ethyl 5,7-dioxo-6-methyloctanoate (**10b**). Ethyl 2-carbethoxy-4,5-dimethyl-1*H*-pyrrole-3-propanoate (**9a**)[14] and ethyl 2-carbethoxy-5-formyl-4-methyl-1*H*-pyrrole-3-propanoate (**8a**)[15] were prepared as described in the literature.

Ethyl 5,7-Dioxo-6-methyloctanoate (10b). To a suspension of anhydrous zinc chloride (40 g, 0.297 mol) in anhydrous dichloromethane (270 mL) was added ethyl glutaroyl chloride (48 g, 0.27 mol) at 0 °C, and the mixture was stirred for an additional 0.5 h. The TMS silyl enol ether of 2-butanone (mixture of silyl 2- and 1-enol ethers) (43 g, 0.297 mol) was added dropwise during 0.5 h at 0 °C, and then the reaction mixture was stirred sequentially for 1 h at 0 °C and then 2 h at room temperature. The brown reaction mixture was poured into water (500 mL), and the mixture was extracted with dichloromethane until the organic extractions were colorless. The combined organic extractions were washed with water (2 × 100 mL) and then with saturated aq NaHCO$_3$ solution (3 × 150 mL, during which the color changed to a beautiful orange) and saturated brine (2 × 100 mL). The organic layer was dried over anhydrous Na$_2$SO$_4$ and concentrated (roto-vap). The residue was distilled under vacuum to remove a low-boiling byproduct (bp < 150 °C, 30 mmHg) to leave a colorless oil (23.5 g, 37% yield) that was pure enough for the next step.

Ethyl 2-(Carbethoxy-4,5-dimethyl-1*H*-pyrrolyl)-3-butanoate (9b). To a solution of ethyl 5,7-dioxo-6-methyloctanoate (**10b**) (15 g, 0.07 mol) in glacial acetic acid (70 mL) was added anhydrous sodium acetate (19 g). Then zinc dust (15 g) was added portionwise with vigorous stirring during which time the temperature was kept under 80 °C. The temperature was raised to 95 °C after the addition of zinc dust was complete, and then a solution of diethyl oximinomalonate (13.1 g, 0.07 mmol) in glacial acetic acid (20 mL) and water (7 mL) was added slowly. The reaction mixture was heated at reflux for 2.5 h and then poured into ice and allowed to stand for 2 h at room temperature. The solid was collected by filtration, washed with water, and dried to give the desired pyrrole: 10 g, 50.8% yield; mp 63−66 °C (lit.[25a] mp 64−65 °C); IR (NaCl, dichloromethane) ν 3424, 3053, 2984, 1721, 1656, 1264, 1261, 739, 705, 669 cm^{-1}; ^{1}H NMR δ 1.24 (t, J = 7.2 Hz, 3H), 1.34 (t, J = 7.2 Hz, 3H), 1.84 (m, J = 7.5 Hz, 2H), 1.86 (s, 3H), 2.18 (s, 3H), 2.30 (t, J = 7.5 Hz, 2H), 2.75 (t, J = 7.5 Hz, 2H), 4.12 (q, J = 7.2 Hz, 2H), 4.29 (q, J = 7.2 Hz, 2H), 8.53 (brs, 1H) ppm; ^{13}C NMR δ 8.6, 11.3, 14.2, 14.4, 24.5, 25.7, 33.9, 59.5, 60.0, 116.5, 129.9, 130.9, 161.6, 173.7 ppm; GC−MS (*m/z*) 281 [M$^+$], 236, 208, 193, 148, 134, 108, 79 amu.

Ethyl (2-Carbethoxy-5-formyl-4-methyl-1*H*-4-pyrrolyl)-4-butanoate (8b). To a solution of ethyl (5-carbethoxy-2,3-dimethyl-1*H*-4-pyrrolyl)-4-butanoate (**9b**) (15 g, 0.051 mol) in THF (536 mL), HOAc (135 mL), and water (536 mL) was added ceric ammonium nitrate (CAN) (120 g, 220 mmol) in one

(31) Harada, N.; Nakanishi, K. *Circular Dichroic Spectroscopy-Exciton Coupling in Organic Stereochemistry*; University Science Books: Mill Valley, CA, 1983.
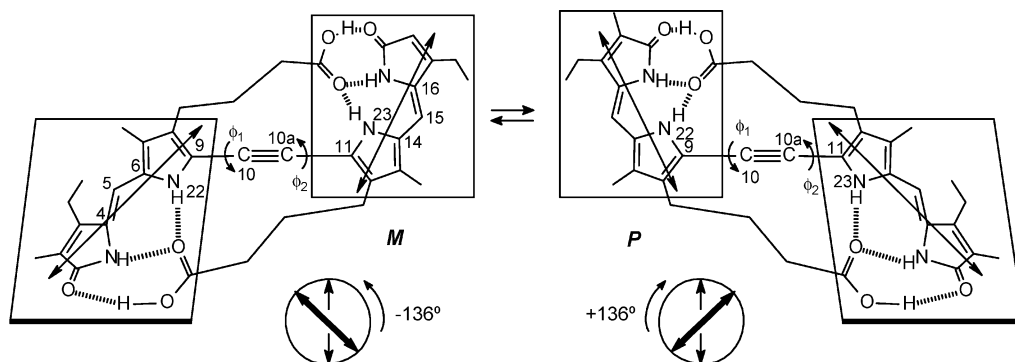
(32) Riegel, B.; Lillienfield, W. M. *J. Am. Chem. Soc.* **1945**, *67*, 1273−1275.

(33) Ahmad, S.; Khan, M. A.; Iqbal, J. *Synth. Commun.* **1988**, *18*, 1679−1683. The silyl enol ether preparation could be scaled up successfully, by a factor of 10−20 while keeping the DMF solvent volume the same as reported.

FIGURE 10. Twisted, intramolecularly hydrogen-bonded enantiomeric conformations of acetylenic rubins with butyric acid chains **M** and **P**. Interconversion is accomplished by rotating about ϕ_1 and ϕ_2. In **M** and **P**, the dipyrrinone chromophores are approximately planar, with torsion angles C(4)−C(5)−C(6)−N(22) and N(23)−C(14)-−(15)−C(16) ∼ 23°, and the angle of intersection of the two planes (dihedral angle, θ) is ∼127° for $\phi_1 \sim \phi_2 \sim 68°$. The double-headed arrows represent the approximate direction and intensity of the dipyrrinone long-wavelength electric transition dipole moments. The relative orientations or helicities (**M**, minus; **P**, plus) of the vectors are shown (inset) for each enantiomer. For these conformations, the **M** dipole helicity correlates with the **M** molecular chirality and the **P** helicity with the **P** molecular chirality.
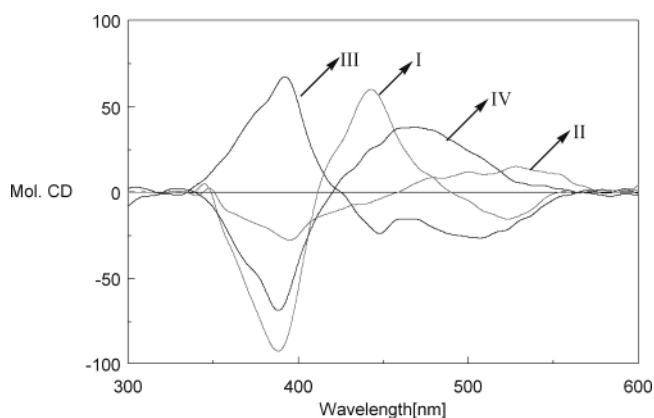

FIGURE 11. Comparison of the circular dichroism (CD) and UV−vis spectroscopic data of **1a** and **1b** in CHCl₃ solutions containing quinine (I and II, pigment concentrated ∼1.4 × 10⁻⁵ M; quinine concentrated ∼4.2 × 10⁻³; pigment/quinine molar ratio = ∼1:300) and in HSA pH 7.4 tris buffer (III and IV, pigment concentrated ∼1.4 × 10⁻⁵ M, HSA concentrated 2.8 × 10⁻⁵ M). Spectrum I: **1a**, CHCl₃ $\Delta\epsilon_{388}^{max}$ −92, $\Delta\epsilon_{412} = 0$, $\Delta\epsilon_{442}^{max}$ +59; UV−vis $\Delta\epsilon_{396}^{max}$ 41 800. Spectrum II: **1b**, CHCl₃ $\Delta\epsilon_{395}^{max}$ −28, $\Delta\epsilon_{459} = 0$, +14; UV−vis $\Delta\epsilon_{396}^{max}$ 48 800. Spectrum III: **1a**, HSA $\Delta\epsilon_{392}^{max}$ +67, $\Delta\epsilon_{425} = 0$, $\Delta\epsilon_{508}^{max}$ −26; UV−vis $\Delta\epsilon_{494}^{max}$ 42 300. Spectrum IV: **1b**, HSA $\Delta\epsilon_{388}^{max}$ −69, $\Delta\epsilon_{420} = 0$, $\Delta\epsilon_{466}^{max}$ +37; UV−vis $\Delta\epsilon_{499}^{max}$ 34 500.

portion. The mixture was stirred at room temperature for 2 h, poured into water (2 L), and extracted with dichloromethane (3 × 800 mL). After the mixture was washed with water (3 × 1000 mL) and saturated aq sodium bicarbonate solution (3 × 300 mL), the combined organic extracts were dried over anhyd Na₂SO₄ and concentrated (roto-vap). The resulting brown oil was purified by passing it through a short column of silica gel using dichloromethane as eluent. After evaporation of the solvent, the residue was recrystallized from chloroform−hexane to afford pure **8b**: 9 g, 60% yield; mp 52−55 °C (lit.[25a] mp 56−57 °C); IR (NaCl, dichloromethane) ν 3448, 3312, 3019, 2984, 1725, 1668, 1438, 1265, 1216, 705, 669 cm-1; ¹H NMR δ 1.25 (t, $J = 7.2$ Hz, 3H), 1.38 (t, $J = 7.2$ Hz, 3H), 1.85 (m, $J = 7.5$ Hz, 2H), 2.32 (s, 3H), 2.34 (t, $J = 7.5$ Hz, 2H), 2.78 (t, $J = 7.5$ Hz, 2H), 4.13 (q, $J = 7.2$ Hz, 2H), 4.36 (q, $J = 7.2$ Hz, 2H), 9.43 (brs, 1H), 9.77 (s, 1H) ppm; ¹³C NMR δ 8.3, 14.2, 14.3, 23.5, 25.4, 33.7, 60.2, 60.9, 124.3, 129.8, 130.0, 130.160.5,7, 173.4, 179.1 ppm; GC−MS (*m/z*) 295 [M⁺•], 249, 222, 207, 180, 148, 120, 65 amu.

(2-Carboxy-5-formyl-4-methyl-1*H*-pyrrolyl)-3-propano-ic Acid (7a). To a solution of pyrrole **8a** (3 g, 10.67 mmol) in THF−H₂O (5:1 by volume, 115 mL) was added LiOH·H₂O (1.78 g, 42.5 mmol, 4 mol equiv). The mixture was stirred at 70 °C for 4 h under N₂ and then cooled to room temperature. The red aqueous layer was washed with ether (3 × 50 mL) and acidified carefully at 0 °C with saturated aq NaHSO₄ solution until the pH was about 3. The mixture was stirred at 0 °C for an additional 30 min until all the oil had solidified. The solid was collected by filtration and washed with a small amount of cold water to afford pyrrole diacid **7a**: 2.04 g, 85% yield; mp >150 °C dec; IR (KBr film) ν 3551, 3254, 1690, 1667, 1545, 1350, 1229, 809, 754 cm⁻¹; ¹H NMR (DMSO-d_6) δ 2.20 (s, 3H), 2.33 (t, $J = 7.5$ Hz, 2H), 2.64 (t, $J = 7.5$ Hz, 2H), 9.71(s, 1H), 12.3 (brs, 2H) ppm; ¹³C NMR (DMSO-d_6) δ 9.42, 19.8, 34.9, 124.8, 126.9, 129.6, 130.7, 162.2, 174.3, 182.2 ppm. Anal. Calcd for C₁₀H₁₁NO₅ (225.2): C, 53.33; H, 4.92; N, 6.22. Found: C, 53.15; H, 5.01; N, 6.24.

(2-Carboxy-5-formyl-4-methyl-1*H*-3-pyrrolyl)-4-butano-ic Acid (7b). Compound **7b** was prepared in 70% yield as described above for (5-carboxy-2-formyl-3-methyl-1*H*-pyrrolyl)-3-propanoic acid **7a**: mp 184 °C dec; IR (KBr film) ν 3550, 3254, 1690, 1667, 1498, 1333, 1258, 948, 754 cm⁻¹; ¹H NMR (DMSO-d_6) δ 1.62 (m, $J = 7.3$ Hz, 2H), 2.13 (t, $J = 7.3$ Hz, 2H), 2.17 (s, 3H), 2.64 (t, $J = 7.3$ Hz, 2H), 9.71 (s, 1H), 12.23 (brs, 2H) ppm; ¹³C NMR (DMSO-d_6) δ 9.49, 18.89, 25.86, 33.61, 124.8, 126.9, 130.4, 130.8, 162.3, 174.7, 182.2 ppm; FAB (3-NBA matrix) HRMS calcd for C₁₁H₁₄NO₅ (M + H⁺, 240.0872), found 240.0878, Δ = 4.2 ppm. Anal. Calcd for C₁₁H₁₃NO₅ (239.2): C, 55.23; H, 5.48; N, 5.86. Anal. Calcd for C₁₁H₁₃NO₅·¹/₂H₂O: C, 53.22; H, 5.68; N, 5.64. Found: C, 53.44; H, 5.57; N, 5.17.

(5-Iodo-2-formyl-3-methyl-1*H*-4-pyrrolyl)-3-propano-ic Acid (6a). To a solution of KI (4.2 g) and iodine (1.72 g) in water (27 mL) was added slowly a solution of pyrrole diacid **7a** (1.52 g, 6.75 mmol) in water (27 mL) containing NaHCO₃ (1.14 g). The reaction mixture was stirred at 65 °C for 1 h and then at reflux for 2 h, during which time carbon dioxide evolved and the color gradually lightened. A yellow solid separated when the reaction mixture was cooled to room temperature. The solid was collected by filtration and washed with cold water to afford iodopyrrole **6a**: 1.24 g, 60% yield; mp 194−196 °C; IR (KBr film) ν 3164, 2916, 1686, 1618, 1425, 1397, 1332, 901, 833 cm⁻¹; ¹H NMR (DMSO-d_6) δ 2.22 (s, 3H), 2.29 (t, $J = 6.9$ Hz, 2H), 2.47 (t, $J = 6.9$ Hz, 2H), 9.35 (s, 1H), 12.1 (brs, 1H), 12.2 (brs, 1H) ppm; ¹³C NMR (DMSO-d_6) δ 9.3, 21.8, 34.6, 83.4, 128.3, 129.4, 133.9, 173.9, 177.2 ppm. Anal. Calcd for C₉H₁₀INO₃ (307.2): C, 35.20; H, 3.28; N, 4.56. Found: C, 35.60; H, 3.30; N, 4.16.

(5-Iodo-2-formyl-3-methyl-1*H*-4-pyrrolyl)-4-butanoic Acid (6b). Compound **6b** was prepared in 60% yield as described above for (5-iodo-2-formyl-3-methyl-1*H*-4-pyrrolyl)-3-propanoic acid **6a**: mp 152−3 °C; IR (KBr film) ν 3164, 2915, 1686, 1673, 1425, 1266, 833 cm^{-1}; ^{1}H NMR (DMSO-d_6) δ 1.57 (m,, $J = 7.2$ Hz, 2H), 2.15 (t, $J = 7.2$ Hz, 2H), 2.28 (t, $J = 7.2$ Hz, 2H), 2.20 (s, 3H), 9.35 (s, 1H), 12.0 (brs, 1H), 12.2 (brs, 1H) ppm; ^{13}C NMR (DMSO-d_6) δ 9.4, 25.3, 25.5, 33.5, 83.4, 100.6, 129.2, 134.0, 174.5, 177.2 ppm. Anal. Calcd for $C_{10}H_{12}$-INO$_3$ (321.2): C, 37.40; H, 3.77; N, 4.36. Found: C, 37.40; H, 4.02; N, 4.05.

Methyl (5-Iodo-2-formyl-3-methyl-1*H*-4-pyrrolyl)-3-propanoate (5a). To a 125 mL Erlenmeyer flask were added aq KOH (2.5 g in 2.5 mL water) and 20 mL of ether. The mixture was cooled to 0 °C, and *N*-methyl-*N*-nitrosourea (0.55 g) was added and stirred slowly for 10 min. The yellow ether layer was poured into a solution of (5-iodo-2-formyl-3-methyl-1*H*-pyrrolyl)-3-propanoic acid **6a** (200 mg, 0.652 mmol) in methanol (15 mL) in two portions during 5 min. The reaction mixture was stirred for another 10 min until no further N$_2$ evolved. Glacial acetic acid (0.5 mL) was then added to destroy excess diazomethane. The mixture was poured into water (50 mL) and extracted with dichloromethane (3 × 50 mL). The combined organic layers were washed with water (2 × 50 mL), saturated NaHCO$_3$ solution (2 × 50 mL), and brine (2 × 50 mL) and then dried over anhydrous Na$_2$SO$_4$. After evaporation of the solvent, the residue was recrystallized from chloroform−hexane to give **5a**: 170 mg, 78% yield; mp 142−144 °C; IR (NaCl, dichloromethane) ν 3432, 2253, 1635, 1412, 1363, 1094, 909, 734, 650 cm^{-1}; ^{1}H NMR δ 2.33 (s, 3H), 2.47 (t, $J = 7.5$ Hz, 2H), 2.72(t, $J = 7.5$ Hz, 2H), 3.69 (s, 3H), 9.11 (brs, 1H), 9.40 (s, 1H) ppm; ^{13}C NMR δ 8.9, 21.6, 34.0, 51.7, 128.1, 128.8, 130.5, 133.9, 172.9, 176.1 ppm; GC−MS (*m*/*z*) 321 [M$^+$], 262, 248, 194, 179, 152, 106, 77 amu. Anal. Calcd for $C_{10}H_{12}$-INO$_3$ (321.1): C, 37.40; H, 3.77; N, 4.36. Found: C, 37.67; H, 3.62; N, 4.06.

Methyl (5-Iodo-2-formyl-3-methyl-1*H*-4-pyrrolyl)-4-butanoate (5b). Compound **5b** was prepared in 90% yield as described above for methyl (5-iodo-2-formyl-3-methyl-1*H*-4-pyrrolyl)-3-propanoate **5a**: mp 124−5 °C; IR (NaCl, dichloromethane) ν 3430, 1635, 1412, 1360, 1095, 909, 732, 649 cm^{-1}; ^{1}H NMR δ 1.79 (m, $J = 7.5$ Hz, 2H), 2.31 (s, 3H), 2.34 (t, $J = 7.5$ Hz, 2H), 2.42 (t, $J = 7.5$ Hz, 2H), 3.67 (s, 3H), 9.40 (s, 1H), 9.40 (brs, 1H) ppm; ^{13}C NMR δ 8.9, 24.9, 25.5, 33.2, 51.5, 80.9, 129.9, 130.2, 133.9, 173.7, 176.0 ppm; GC−MS (*m*/*z*) 335 [M$^{+\bullet}$], 276, 248, 208, 180, 148, 120, 65 amu. Anal. Calcd for $C_{11}H_{14}$-INO$_3$ (335.1): C, 39.42; H, 4.21; N, 4.18. Found: C, 39.58; H, 4.16; N, 4.18.

Methyl (2-Formyl-3-methyl-5-(trimethylsilyl)ethynyl-1*H*-4-pyrrolyl-3-propanoate (4a). To a solution of methyl (5-iodo-2-formyl-3-methyl-1*H*-4-pyrrolyl-3-propanoate (**5a**) (295 mg, 0.92 mmol) in diethylamine (9.5 mL) were added under N$_2$ (trimethylsilyl)acetylene (0.138 g, 1.38 mmol), dichlorobis-(triphenyphosphine)palladium(II) (11.5 mg, 0.016 mmol), and copper(I) iodide (5.98 mg, 0.032 mmol). The homogeneous mixture was stirred at 50 °C for 1 h, during which time the color became yellow and a brown oil separated. After evaporation of the solvent under vacuum, the residue was subjected to chromatography on a short column of silica gel using dichloromethane−hexane (2:1) as eluent. After evaporation of the solvent, the residue was recrystallized from hexane−chloroform to give pure pyrrole **4a**: 240 mg, 90% yield; mp 92−3 °C; IR (NaCl, dichloromethane) ν 3441, 2253, 1731, 1644, 1447, 1379, 1251, 1094, 848, 732, 650 cm^{-1}; ^{1}H NMR δ 0.25 (s, 9H), 2.28 (s, 3H), 2.57 (t, $J = 7.5$ Hz, 2H), 2.82 (t, $J = 7.5$ Hz, 2H), 3.68 (s, 3H), 8.95 (brs, 1H), 9.58 (s, 1H) ppm; ^{13}C NMR δ −0.34, 8.5, 19.8, 33.9, 51.5, 94.6, 103.0, 118.7, 129.1, 129.4, 130.2, 173.1, 177.0 ppm; GC−MS (*m*/*z*) 291 [M$^{+\bullet}$], 260, 218, 204, 158, 130, 89, 73 amu. Anal. Calcd for $C_{15}H_{21}NO_3Si$ (291.2): C, 61.82; H, 7.26; N, 4.81. Found: C, 62.12; H, 7.50; N, 4.94.

Methyl (2-Formyl-3-methyl-5-(trimethylsilyl)ethynyl-1*H*-pyrrolyl-4-butanoate (4b). Compound **4b** was prepared in 80% yield as described above for methyl (2-formyl-3-methyl-5-(trimethylsilyl)ethynyl-1*H*-4-pyrrolyl-3-propanoate **4a**: mp 64−5 °C; IR (NaCl, dichloromethane) ν 3441, 1730, 1647, 1445, 1094, 906, 732, 650 cm^{-1}; ^{1}H NMR δ 0.25 (s, 9H), 1.85 (m, $J = 7.5$ Hz, 2H), 2.27 (s, 3H), 2.33 (t, $J = 7.5$ Hz, 2H), 2.53 (t, $J = 7.5$ Hz, 2H), 3.66 (s, 3H), 8.88 (brs, 1H), 9.58 (s, 1H) ppm; ^{13}C NMR δ −0.28, 8.5, 23.1, 24.9, 33.3, 51.4, 94.8, 102.6, 118.7, 129.2, 129.4, 130.1, 173.8, 177.0 ppm; GC−MS (*m*/*z*) 305 [M$^{+\bullet}$], 274, 218, 202, 172, 144, 88, 73 amu. Anal. Calcd for $C_{16}H_{23}$-NO$_3$Si (305.4): C, 62.92; H, 7.59; N, 4.59. Found: C, 62.70; H, 7.38; N, 4.86.

Methyl (2-Formyl-3-methyl-5-ethynyl-1*H*-4-pyrrolyl)-3-propanoate (3a). To a solution of pyrrole **4a** (70 mg, 0.24 mmol) in THF (3 mL) was added n-Bu$_4$NF (1.0 M THF solution, 0.25 mL). The mixture was stirred at room temperature for 1 h, and the color darkened. After removal of the solvent under reduced pressure, the residue was passed through a short column of silica gel using dichloromethane−hexane (3:1 by volume) as eluent to give a yellow solution. After evaporation of the solvent, **3a** was obtained as a pale yellow solid: 50 mg, 85% yield; mp 129−130 °C; IR (NaCl, dichloromethane) ν 3441, 2252, 1647, 1378, 1094, 907, 737 650 cm^{-1}; ^{1}H NMR δ 2.30 (s, 3H), 2.57 (t, $J = 7.5$ Hz, 2H), 2.84 (t, $J = 7.5$ Hz, 2H), 3.46 (s, 1H), 3.68 (s, 3H), 9.08 (brs, 1H), 9.60 (s, 1H) ppm; ^{13}C NMR δ 8.5, 19.7, 34.0, 51.6, 74.0, 84.5, 117.6, 129.3, 129.4, 129.5, 173.1, 177.3 ppm; GC−MS (*m*/*z*) 219 [M$^{+\bullet}$], 160, 146, 132, 103, 77, 51 amu. Anal. Calcd for $C_{12}H_{13}NO_3$ (219.2): C, 65.74; H, 5.98; N, 6.39. Found: C, 65.92; H, 6.18; N, 6.42.

Methyl (2-Formyl-3-methyl-5-ethynyl-1*H*-pyrrolyl-4-butanoate (3b). Compound **3b** was prepared in 85% yield as described above for methyl (2-formyl-3-methyl-5-ethynyl-1*H*-pyrrolyl-3-propanoate (**3a**): mp 88−9 °C; IR (NaCl, dichloromethane) ν 3443, 2250, 1648, 1370, 1094, 907, 737 649 cm^{-1}; ^{1}H NMR δ 1.87 (m, $J = 7.5$ Hz, 2H), 2.28 (s, 3H), 2.33 (t, $J = 7.5$ Hz, 2H), 2.55 (t, $J = 7.5$ Hz, 2H), 3.43 (s, 1H), 3.66 (s, 3H), 9.16 (brs, 1H), 9.60 (s, 1H) ppm; ^{13}C NMR δ 8.5, 23.5, 25.0, 33.2, 51.4, 74.3, 84.1, 117.9, 129.4, 129.7, 130.3, 173.8, 177.3 ppm; GC−MS (*m*/*z*) 233 [M$^{+\bullet}$], 202, 174, 146, 130, 117, 77, 65 amu. Anal. Calcd for $C_{13}H_{15}NO_3$ (233.2): C, 66.94; H, 6.48; N, 6.00. Found: C, 66.65; H, 6.59; N, 5.71.

1,2-Bis(3-methoxycarbonylethyl-4-methyl-5-formyl-2-pyrrolyl) (2a). To a solution of pyrrole **3a** (103 mg, 0.47 mmol) and pyrrole **5a** (154 mg, 0.48 mmol) in diethylamine (4.8 mL) were added dichlorobis(triphenyphosphine)palladium(II) (5.9 mg, 0.008 mmol) and copper(I) iodide (3.0 mg, 0.016 mmol) under an N$_2$ atmosphere. The mixture was stirred at 50 °C for 3 h. The final brown solution was evaporated under vacuum to remove all of the solvent. The residue was passed through a short column of silica gel using dichloromethane and ethyl acetate (2:1, v/v) as eluent. All of the yellow eluent was collected. After the solvent was evaporated (roto-vap), the yellow solid was recrystallized from hot ethyl acetate to afford acetylenic dipyrrole dialdehyde **2a** as yellow crystals: 116 mg, 60% yield; mp > 216 °C dec; IR (KBr) ν 3216, 1741, 1731, 1625, 1614, 1452, 1396, 1278, 1198, 1175, 668 cm^{-1}; ^{1}H NMR δ 2.33 (s, 6H), 2.60 (t, $J = 7.5$ Hz, 4H), 2.89 (t, $J = 7.5$ Hz, 4H), 3.67 (s, 6H), 9.64 (s, 2H) ppm; ^{1}H NMR (DMSO-d_6) δ 2.22 (s, 6H), 2.49 (t, $J = 7.5$ Hz, 4H), 2.73 (t, $J = 7.5$ Hz, 4H), 3.52 (s, 6H), 9.57 (s, 2H), 12.27 (brs, 2H) ppm; ^{13}C NMR (DMSO-d_6) δ 9.0, 19.8, 34.3, 71.7, 86.5, 117.7, 128.9, 129.1, 130.4, 172.9, 178.7 ppm. Anal. Calcd for $C_{22}H_{24}N_2O_6$ (412.1): C, 64.07; H, 5.87; N, 6.79. Found: C, 63.91; H, 5.87; N, 6.79.

1,2-Bis(3-methoxycarbonyl-*n*-propyl-4-methyl-5-formyl-2-pyrroyl)ethyne (2b). Compound **2b** was prepared in 40% yield as described for **2a**, by the condensation of pyrrole **3b** and **5b**: mp > 185 °C dec; IR (KBr) ν 3211, 1740, 1727, 1625, 1452, 1391, 1278, 1190, 1175, 666 cm^{-1}; ^{1}H NMR δ 1.89 (m, $J = 7.5$ Hz, 4H), 2.29 (s, 6H), 2.42 (t, $J = 7.5$ Hz, 4H), 2.56 (t, $J = 7.5$ Hz, 4H), 3.78 (s, 6H), 9.63 (s, 2H), 9.95 (brs, 2H) ppm;

^{13}C NMR δ 8.5, 23.7, 25.1, 33.2, 51.9, 80.3, 116.9, 129.3, 130.3, 132.9, 173.7, 177.3 ppm; FAB HRMS (3-NBA matrix) calcd for $(M + H)^+$ $C_{24}H_{29}N_2O_6$ (441.2026), found 441.2017 (1.9 ppm).

10,10a-Didehydro-10a-homomesobilirubin-XIIIα (Bis-(2,7-dimethyl-3-ethyl-8-carboxyethyldipyrrin-1(10*H***)-on-9-yl)acetylene) (1a).** To a solution of acetylenic dipyrrole dialdehyde **2a** (58 mg, 0.14 mmol) and pyrrolinone **13** (176 mmol, 1.4 mmol, 10 mol equiv) in methanol (24 mL) and H_2O (6 mL) was added KOH (2.95 g) under N_2. The mixture was stirred at reflux for 60 h, during which time the color was changed from pale yellow to red and then to red-black. The solution was cooled to 0 °C and acidified slowly using saturated sodium bisulfate solution. The precipitate was collected by filtration and washed with cold water. Further purification was reached through dissolving the solid in a small amount of pyridine and then adding methanol and ether to facilitate the precipitation. The final product was obtained as a red solid after repeating this procedure three times: 34 mg, 40% yield; mp >280 °C dec; IR (KBr) ν 3386, 3329, 2970, 2917, 1711, 1649, 1625, 1614, 1558, 1268, 1172, 706, 668 cm^{-1}; ^{1}H NMR (DMSO-d_6, 500 MHz) δ 1.10 (t, $J = 7.5$ Hz, 6H), 1.79 (s, 6H), 2.07 (s, 6H), 2.37 (t, $J = 7.5$ Hz, 4H), 2.53 (q, $J = 7.5$ Hz, 4H), 2.69 (t, $J = 7.5$ Hz, 4H), 5.93 (s, 2H), 10.11 (brs, 2H), 11.18 (brs, 2H), 12.14 (brs, 2H) ppm; ^{13}C NMR data are in Table 1 and UV–vis data are in Table 4. Anal. Calcd for $C_{34}H_{38}N_4O_6$ (598.6): C, 68.21; H, 6.40; N, 9.36. Anal. Calcd for $C_{34}H_{38}N_4O_6 \cdot CH_3OH$ (640.6): C, 66.65; H, 6.71; N, 8.88. Found: C, 66.47; H, 6.56; N, 8.48.

10,10a-Didehydro-10a-homo-8,12-bis-homomesobilirubin-XIIIα (Bis(2,7-dimethyl-3-ethyl-8-carboxypropyldipyrrin-1(10*H***)-on-9-yl)acetylene) (1b).** Compound **1b** was prepared in 30% yield as described above for **1a**. An analytical sample was purified by radial chromatography using CH_2Cl_2 and CH_3OH as eluent (50:1, by volume): mp >320 °C dec; IR (KBr) ν 3380, 3055, 2968, 2306, 1703, 1422, 1265, 1151, 896, 789, 705 cm^{-1}; ^{1}H NMR (DMSO-d_6, 500 MHz) δ 1.10 (t, $J = 7.5$ Hz, 6H), 1.73 (m, $J = 7.5$ Hz, 4H), 1.80 (s, 6H), 2.07 (s, 6H), 2.21 (t, $J = 7.5$ Hz, 4H), 2.51 (q, $J = 7.5$ Hz, 4H), 2.54 (t, $J = 7.5$ Hz, 4H), 5.95 (s, 2H), 10.03 (brs, 2H), 11.03 (brs, 2H), 12.03 (brs, 2H) ppm; ^{13}C NMR data are in Table 1 and UV–vis data in Table 4. Anal. Calcd for $C_{36}H_{42}N_4O_6$ (626.7): C, 68.99; H, 6.75; N, 8.94. Anal. Calcd for $C_{36}H_{42}N_4O_6 \cdot H_2O$ (644.7): C, 67.06; H, 6.87; N, 8.68. Found: C, 67.38; H, 6.52; N, 8.29.

Supporting Information Available: Computed[26] atomic coordinates of **1a** and **1b** of Figure 5 are provided. This material is available free of charge via the Internet at http://pubs.acs.org.

JO030252T